

Induced quantum magnetism on a triangular lattice of non-Kramers ions in $\text{PrMgAl}_{11}\text{O}_{19}$

S. Kumar,^{1,2} M. Klicpera,¹ A. Eliáš,¹ M. Kratochvílová,¹ K. Załęski,³ M. Śliwińska-Bartkowiak,² R. H. Colman,¹ and G. Bastien^{1*}

¹ Charles University, Faculty of Mathematics and Physics, Department of Condensed Matter Physics, Prague, Czech Republic

² Adam Mickiewicz University, Faculty of Physics and Astronomy, Department of Experimental Physics of Condensed Phase, Poznan, Poland

³ Adam Mickiewicz University, NanoBioMedical Centre, Poznan, Poland

*Corresponding author: gael.bastien@matfyz.cuni.cz

Abstract

We report the magnetic properties of the quantum triangular lattice antiferromagnet (TLAF) $\text{PrMgAl}_{11}\text{O}_{19}$ through magnetization and specific heat measurements. Strong magnetic anisotropy indicates the realization of an Ising-like magnetism in $\text{PrMgAl}_{11}\text{O}_{19}$ single crystal while no long-range magnetic ordering is realized down to 0.4 K. The splitting of the low-lying quasi-doublet into two singlets suggested by experimental data, is consistent with an effective pseudospin-1/2 scenario. The observed gapless excitations in zero field are attributed to induced quantum magnetism, they would be induced by magnetic interactions of an energy scale comparable with the splitting between the two singlets. Based on these results, we modeled the magnetic ground state of $\text{PrMgAl}_{11}\text{O}_{19}$ by a quantum Ising magnet with an intrinsic transverse field rather than a quantum spin liquid (QSL). In addition, our data show a non-monotonous response of the low-temperature specific heat to the external fields revealing a complex interplay between intrinsic and external magnetic fields.

Introduction

The exploration of quantum magnetism has emerged as a significant theme in condensed matter physics, driven by the quest to discover exotic states of matter that harbor non-local topological excitations or quantum entanglement. So far, the research in quantum magnetism has largely focused on systems with spin or effective spin-1/2 moments, where the formation of quantum spin liquids (QSLs) is anticipated [1-3]. However, recent studies have revealed that frustrated magnets with integer spin S or total angular momentum J can also host a rich variety of quantum magnetic phases, including quantum Ising magnets [4-11], quantum nematic phases [12-14], quadrupolar orders [15-17], intertwined dipolar-multipolar orders [18, 19], as well as disordered dipolar-multipolar states [20].

Frustrated magnets involving non-Kramers rare earth ions such as Pr^{3+} and Tm^{3+} with $J = 4$ and $J = 6$ are promising platforms for the study of these exotic phases [5, 9, 10, 21]. The crystal electric field (CEF) splitting isolates a quasi-doublet ground state. Since Pr^{3+} and Tm^{3+} do not adhere to Kramers' theorem, this ground state further splits into two singlets. In the case of Pr^{3+} , the two energy levels are [9, 21]:

$$\begin{aligned} |0\rangle &= |J_z = +4\rangle + |J_z = -4\rangle \\ |1\rangle &= |J_z = +4\rangle - |J_z = -4\rangle \end{aligned} \quad (1)$$

It is important to note that both energy levels correspond to states with zero magnetic moment whilst finite magnetic moment can be achieved upon the mixture of the two levels [4, 5, 6, 9, 21-24]. These two levels also carry multipolar moments [18,19], which can lead to the formation of an uncommon magnetic order combining dipolar with higher order multipolar orders [18], as observed in the triangular magnet TmMgGaO_4 [19]. In TmMgGaO_4 , the magnetic order forms upon a double phase transition including a topological Berezinskii-Kosterlitz-Thouless (BKT) phase transition [7, 25-27]. When the energy splitting between the two singlets, h , is comparable to the magnetic interaction, J , the magnetism can be described by an effective Hamiltonian on pseudospins $S = \frac{1}{2}$ [4, 5, 6, 9, 21, 28]. The energy splitting h is equivalent to an intrinsic transverse field acting on the pseudospin component S^x and the Hamiltonian can be written as:

$$H = \sum_{\langle i,j \rangle} JS_i^z S_j^z - \sum_i h S_i^x - \sum_i \mu_0 \mu_B g_c H S_i^z. \quad (2)$$

Theoretical studies of this Hamiltonian revealed that the transverse field induces quantum fluctuations in Ising magnets [6-8, 21, 25, 29]. In the case of the triangular magnet, the classical spin liquid state arising at the pure Ising limit [30, 31] is replaced by a quantum state, the clock order under the presence of an intrinsic transverse field [6 – 8, 18, 27, 29]. This state harbors two types of topological excitation: string and spinon [7, 8]. The clock order vanishes at a quantum critical point at $h_c = 0.8 J$ [6 – 8, 27, 29]. Beyond, this critical value, the pseudospins are mainly polarized by the intrinsic transverse field, however, gapless magnetic excitations arise from the proximity to quantum criticality and imply a power law behavior of the low-temperature specific heat [9, 10].

Recently, the triangular magnets $\text{PrZnAl}_{11}\text{O}_{19}$ and $\text{PrMgAl}_{11}\text{O}_{19}$ were proposed as QSL candidates [32-39]. Their crystal structure is close to the two-dimensional limit with the planar triangular lattice of the non-Kramers ion Pr^{3+} [32-34]. Structural disorder is induced by the mixture of Mg/Zn and Al on one of the Al sites and by anomalous displacement of another Al site and Pr site [37]. Magnetization measurements on single crystals of $\text{PrMgAl}_{11}\text{O}_{19}$ revealed the proximity to the Ising limit [36-39]. Specific heat measurements excluded the formation of magnetic order down to 0.1K [36-39]. The low-temperature specific heat in zero field follows a power-law behavior that can be fitted nearly to a T^2 dependence in the temperature range 0.4 to 2 K. However, above 0.5 T, a deviation from this power law is observed, which may indicate the formation of an

energy gap [36-39]. In addition, powder inelastic scattering revealed an excitation at 1.5 meV, interpreted as an excitation of CEF level [36].

In this paper, we propose reconsidering the interpretation of the magnetic properties of $\text{PrMgAl}_{11}\text{O}_{19}$. By employing magnetic susceptibility, isothermal magnetization, and specific heat measurements on high-quality single crystals grown by the floating zone method, we confirm the proximity to Ising behavior and the absence of magnetic order. Based on our detailed study of the response of specific heat to the external magnetic field, we argue that the non-Kramers magnet $\text{PrMgAl}_{11}\text{O}_{19}$ is better described as a realization of an Ising triangular lattice antiferromagnet with an intrinsic transverse field rather than a QSL candidate. The TLAF structure and the non-Kramers nature of ions like Pr^{3+} provide fertile ground for exploring the interplay between magnetic frustration, quantum fluctuations, and intrinsic transverse field. In addition, we point out the strong difference in magnetization and specific heat values between the different studies on $\text{PrMgAl}_{11}\text{O}_{19}$ single crystal, which indicated an unresolved dependence on growth conditions.

Methods

The synthesis and subsequent crystal growth of $\text{PrMgAl}_{11}\text{O}_{19}$ were successfully carried out using a solid-state reaction and the optical floating zone (OFZ) method. Initial precursor binary oxides (Pr_6O_{11} , MgO , and Al_2O_3 of 99.99% purity) were initially calcined at 800°C for 24 hours to remove moisture contamination. Following calcination, the oxides were weighed in stoichiometric ratio, thoroughly mixed, and ground to ensure homogeneity of the mixture. The mixture was then pressed into cylindrical rods with dimensions of 6 mm in diameter and 100 mm in length. Densification was achieved using a quasi-hydrostatic pressure of 2 tons for 15 minutes. The resulting rods were sintered in air at 1200°C for 72 hours to promote solid-state reactions and improve the density of the material. The initial attempt to grow $\text{PrMgAl}_{11}\text{O}_{19}$ crystals was conducted using a four-mirror optical floating zone furnace in a reducing environment. This approach, however, encountered issues with the strong evaporation of MgO , which hindered the successful growth of the crystals. In the subsequent attempts, growth was performed under an air atmosphere with a slight overpressure of 1 atm and a flow rate of 3 L/min. The sintered rods were used both as feed and seed material for crystal growth. The feed and seed rods were counter-rotated during the growth at 30 rpm to improve temperature distribution and material mixing in the molten zone. The growth rate was maintained at 2 mm/h. Further details about the used synthesis method have been recently reported in our publication [49-50]. The growth resulted in a green ingot containing multiple grains and grain boundaries were visible to the eyes. The grains were separated using a wire saw and by breaking the ingot and they were identified as single crystals using backscattered Laue X-ray diffraction. A single grain piece was crushed and checked by powder diffraction using a Panalytical Empyrean diffractometer with $\text{CuK}\alpha$ radiation in a capillary transmission parallel beam geometry. Rietveld refinement confirmed the previously proposed magnetoplumbite structure, with lattice parameters $a = 5.58089(7)$ Å and $c = 21.9156(4)$ Å. X-ray fluorescence spectroscopy was used to confirm the compositional cation ratios of the prepared crystal, using an

EDAX Orbis spectrometer with an Rh anode source ($E_{K\alpha} = 20.216$ keV) and polycapillary focusing optics. The DC magnetic susceptibility was measured using a Quantum Design SQUID Magnetic Property Measurement System (MPMS) and a Vibrating Sample Magnetometer (VSM) on a Physical Property Measurement System (PPMS). While specific heat measurements show similar results between samples grown with the two different atmospheres, single-crystal magnetization could be measured only on crystals grown in air. Multiple pieces of single crystals from two growths were used for the bulk measurements with the results proving the sample quality and reproducibility of response. This paper shows the results obtained from a piece of 29.7 mg. $\text{LaMgAl}_{11}\text{O}_{19}$ single crystals were also grown in the air using the floating zone method and their specific heat measurement was used to isolate the magnetic contribution (C_m) Pr-counterpart. Crystals of $\text{LaMgAl}_{11}\text{O}_{19}$ contain a tiny amount of magnetic impurities influencing the specific heat at low-temperature, therefore in the low-temperature limit, the phononic background was obtained from a T^3 extrapolation of the measured specific heat of $\text{LaMgAl}_{11}\text{O}_{19}$.

Results

Magnetization measurements

The magnetic susceptibility of $\text{PrMgAl}_{11}\text{O}_{19}$ was measured along and perpendicular to the c -axis in a magnetic field of 1 T as a function of temperature (Fig. 1a, and 1b). The susceptibility in the field applied along the c -axis follows the Curie-Weiss (CW) law below 80 K. At higher temperatures it deviates from CW behavior, likely due to the influence of excited CEF levels [3, 5]. A CW fitting in the 30-80 K temperature range yields a CW temperature of $\theta_{\text{CW}} = -11$ K in agreement with previous reports [34, 36, 37]. This value implies a magnetic interaction of $J = -2k_B\theta_{\text{CW}}/3 = 0.63$ meV. The CW fit gives the effective magnetic moment $\mu_{\text{eff}} = 4.3 \mu_B$. Assuming a description in terms of pseudospins $S = 1/2$, it implies an effective g -factor of $g_c = 5.0$. The agreement of this value with previous Electron Spin Resonance (ESR) measurements giving $g_c = 5.1$ [37] strongly supports the description of magnetism of $\text{PrMgAl}_{11}\text{O}_{19}$ in terms of pseudospins $S = 1/2$. In contrast, the susceptibility measured with an applied field in the ab -plane (Fig. 1b) is significantly lower (approx. 20-fold at 2 K) compared to the c -axis direction. It does not follow the Curie-Weiss law indicating significant contributions from excited CEF levels.

The isothermal magnetization of $\text{PrMgAl}_{11}\text{O}_{19}$ was measured with the magnetic field applied along the c -axis and within the ab -plane at temperatures between 2 K and 30 K, and in a field up to 14 T (Fig. 1c). The results confirm significant magnetic anisotropy in the crystal, with the magnetization along the c -axis being substantially higher than in the ab -plane. In the ab -plane, the magnetization curves are nearly linear across the measured field range, indicating a paramagnetic response without signs of saturation. In contrast, the magnetization measured with a field along the c -axis deviates from linearity in a relatively small field. Despite this deviation, the magnetization does not saturate up to 14 T. This anisotropic behavior indicates $\text{PrMgAl}_{11}\text{O}_{19}$ is an effective Ising magnet, where the magnetic moments preferentially align along the c -axis, perpendicular to the well separated triangular lattice planes.

We highlight an important non-reproducibility of the magnetization of PrMgAl₁₁O₁₉ grown by different groups. All single crystals we investigated (two ingots grown in air and several single-grain pieces separated from each) reveal similar magnetization values. In contrast, independent studies on several crystals being synthesized using similar floating zone methods reported higher magnetization values. As an example, the magnetization measured at 2 K with a magnetic field applied along the c-axis reaches a value of 1.2 $\mu\text{B}/\text{Pr}$ (our work) at 7 T, while the values of 1.8 $\mu\text{B}/\text{Pr}$ ([36] and [37]), 1.5 $\mu\text{B}/\text{Pr}$ [38] and 1.6 $\mu\text{B}/\text{Pr}$ [39] have also been reported.

Specific Heat

The specific heat of PrMgAl₁₁O₁₉ and its non-magnetic analog LaMgAl₁₁O₁₉ are represented in Fig.2. The absence of any sharp anomaly down to 0.4 K indicates that no long-range magnetic order is present within this temperature range. C_m/T vs T curve at zero field shows a broad hump with a maximum at 5 K and a shoulder at 13 K (Fig. 2b). This double hump structure is also visible in previous single crystal studies of PrMgAl₁₁O₁₉ with variable relative amplitudes of the two humps. We propose that this entropy change actually corresponds to the population of the excited singlet $|1\rangle$, as seen in Pr₂NiTiO₆, TmMgGaO₄, and Pr₃WBO₉ [4, 5, 9] rather than the formation of correlations between magnetic moments has been proposed in [36-39]. This scenario is further confirmed by the previous observation of a Q-independent excitation at 1.5 meV by inelastic neutron scattering on the powder sample [36]. Indeed, such excitation should lead to a Schottky anomaly in the specific heat with a maximum of C_m/T at $T = 5.4$ K in good agreement with our specific heat measurement. The broadness of the hump of C_m/T vs T compared to the Schottky model and the presence of a shoulder around $T = 13$ K could be explained by a strong sensitivity of the energy splitting between the singlet h to structural disorder as previously observed in Pr₂NiTiO₆ and TmMgGaO₄ [4,5].

As an external magnetic field is applied along the easy magnetization axis c , these humps shift to higher temperatures and merge into a single hump above 5 T. Their shift can be explained by the addition of the Zeeman energy to the intrinsic transverse field, increasing the splitting between the energy levels of the pseudo-doublet [6, 9]. The integral of combined humps gives a change of the magnetic entropy of about $R\ln 2$, consistent with a two-level system (Fig. 2c). It further confirms that PrMgAl₁₁O₁₉ can be described as a pseudospin $\frac{1}{2}$ quantum Ising magnet by the Hamiltonian (2). The magnetic contribution to the specific heat at zero field follows a power law behavior $C_m = cT^\alpha$, with $\alpha = 1.9$ on the temperature range $0.5\text{K} < T < 2\text{K}$ (Fig. 4b). This nearly quadratic behavior excludes the formation of an excitation gap of the order of the intrinsic transverse field $h \sim 1.5\text{meV}$; similarly as in other magnets with non-Kramers ions such as Pr₃WBO₉ [9] and KTmSe₂ [10]. At $T = 0$, only the lowest singlet $|0\rangle$ state is populated. Upon increasing temperature the higher singlet $|1\rangle$ state starts gradually to be populated. The antiferromagnetic interaction J favors the population of the highest singlet $|1\rangle$ on neighboring sites, such that magnetic moments arise promoting antiferromagnetic correlations. This

phenomenon leads to collective excitations implying a power law behavior of $C_m(T)$ [9] and is referred to as induced quantum magnetism [21].

Theoretical studies of the quantum Ising magnetism on a triangular lattice predicted the competition between three different magnetic states: the clock order, the up-up-down order and the disordered state [5, 6, 8]. Representation of these phases' magnetic moment configurations, as well as their pseudospin representations, are shown in Fig.3. These phases have previously localized on the transverse field - external field (h - H) phase diagram by quantum Monte Carlo calculations [6]. In the absence of an external field, the magnetic quantum critical point between the clock order and the disordered state is located at $h_c/J \sim 0.8$ [6, 8]. With $h \sim 1.5$ meV and $J \sim 0.6$ meV, PrMgAl₁₁O₁₉ is located around $h/J \sim 2.4$, which is above the critical value, in the regime where magnetic order is not expected.

For further insight into the quantum-induced magnetism in PrMgAl₁₁O₁₉, we investigated the response of the low-temperature specific heat under an external magnetic field applied along the easy magnetization axis c (Fig. 4a). This study revealed a non-monotonic behavior with an increase of the low-temperature specific heat as a function of the magnetic field up to $\mu_0H = 0.25$ T. While the antiferromagnetic interactions favor induced moments with antiferromagnetic correlations, the external magnetic field favors induced moments along the direction of the field. Both can be satisfied by the formation of short-range up-up-down correlations. Therefore, the increase in specific heat with an applied magnetic field up to $\mu_0H = 0.25$ T could be explained by temperature-induced magnetic moments with up-up-down correlations. It should be noticed that the critical intrinsic transverse field h_c was also predicted to show a non-monotonous behavior as a function of the external magnetic field [6], related to the replacement of the clock order by an up-up-down long-range order (Fig. 3) [5, 6, 26, 40]

Above $\mu_0H = 0.25$ T, C_m decreases with magnetic field. It must come from the formation of induced dipolar moments with ferromagnetic correlations preventing short-range antiferromagnetic correlations. However, the magnetic contribution to the specific heat is not fully suppressed and a nearly field-independent component remains. This was previously observed in other studies, which failed to explain it within the assumption that PrMgAl₁₁O₁₉ is a QSL [38, 39]. Considering the specificity of the Pr³⁺ non-Kramers ion, we propose that the magnetic contribution to the low-temperature specific heat could be the sum of a contribution from the induced dipolar moment and a contribution from the multipolar degree of freedom of the singlet ground state [18, 19, 40]. While the external magnetic field suppresses the contribution from dipolar moments, the contribution from the multipolar degree of freedom would remain. In this context, a question remains for future theoretical studies, whether the apparent T^2 behavior of low-temperature specific heat in a high magnetic field of $\mu_0H = 9$ T is compatible with this scenario.

Discussion

Our analysis of the magnetization and the specific heat indicates that PrMgAl₁₁O₁₉ would be a realization of a quantum Ising magnet rather than a quantum spin liquid as previously proposed

[34, 36-39]. Numerous Pr^{3+} and Tm^{3+} based triangular magnets such as CsPrSe_2 [41], PrZn_3P_3 [42], $\text{PrTa}_7\text{O}_{19}$ [43], $\text{Pr}_2\text{O}_2\text{CO}_3$ [44] and $\text{NaBaTm}(\text{BO}_3)_2$ [45] show Van Vleck paramagnetism and suppression of the magnetic contribution to the specific heat at low temperature. These features indicate that the splitting of the quasi-doublet strongly overcomes the magnetic interactions. On the contrary $\text{PrMgAl}_{11}\text{O}_{19}$ with $h/J \sim 2.4$, is much closer to the quantum critical point at $h_c/J = 0.8$ than these Van Vleck paramagnets and even closer than other compounds, e.g. KTmSe_2 with $h/J \sim 3.9$ [10]. In addition, $\text{PrMgAl}_{11}\text{O}_{19}$ shows a large difference between the value of the intrinsic field h and the first CEF excitation Δ as shown qualitatively by our specific heat and quantitatively from the previous point charge calculation ($h/\Delta = 0.05$) [36]. As a consequence, the interplay between the intrinsic transverse field and the CEF excitations can be neglected in $\text{PrMgAl}_{11}\text{O}_{19}$ in contrast to NaTmSe_2 [46], KTmSe_2 [10] and $\text{PrZnAl}_{11}\text{O}_{19}$ [35]. Thus $\text{PrMgAl}_{11}\text{O}_{19}$ is a promising compound for the study of disordered induced quantum magnetism in the vicinity of the quantum critical point. We suggest that the search for a QSL induced by the proximity of the Ising limit should rather be focused on Kramers magnets with effective spin $S_{\text{eff}} = 1/2$ such as $\text{NdTa}_7\text{O}_{19}$ [47].

We also pointed out a strong sample dependence between the different single-crystal studies of the magnetic properties of $\text{PrMgAl}_{11}\text{O}_{19}$ [36-39]. All these studies were based on crystals grown by the floating zone method. The main difference between the growth seems to be the choice of the atmosphere between air in this work and [36, 39], and Ar in [37, 38]. However, there is no apparent correlation between the choice of the atmosphere and magnetic properties. The sample dependence might come from Pr^{3+} vacancies, oxygen vacancies, or the presence of Pr^{4+} impurities. Detailed studies of the magnetic properties of $\text{PrMgAl}_{11}\text{O}_{19}$ depending on growth conditions are desirable.

Conclusion

In conclusion, we successfully grew single crystals of the QSL candidate $\text{PrMgAl}_{11}\text{O}_{19}$ with the floating zone method and performed magnetization and specific heat measurements on them. Based on our results we describe the magnetism of $\text{PrMgAl}_{11}\text{O}_{19}$ as a quantum Ising magnetism that is well described by the intrinsic transverse field model, not the previously proposed QSL state. We claim that $\text{PrMgAl}_{11}\text{O}_{19}$ is a promising compound for the study of quantum Ising magnetism on a triangular lattice. It lies in the regime of quantum-disordered magnetism, where the intrinsic transverse field is strong enough to prevent the formation of magnetic order yet is weak enough to promote the formation of magnetic correlations. The magnetic ground state of $\text{PrMgAl}_{11}\text{O}_{19}$ would deserve further investigation. In particular, single-crystal inelastic neutron scattering would be valuable to study the magnetic excitation of this exotic phase.

Acknowledgment

We acknowledge funding from the Charles University in Prague within the Primus research program with grant number PRIMUS/22/SCI/016. Crystal growth, structural analysis, and magnetic properties measurements were carried out in the MGML (<http://mgml.eu/>), supported within the Czech Research Infrastructures program (project no. LM2023065). We acknowledge

Martin Míšek and Martin Žáček for their technical help with magnetization measurements with VSM technique.

References

- [1] W. Liu *et al.*, “Rare-Earth Chalcogenides: A Large Family of Triangular Lattice Spin Liquid Candidates,” *Chinese Physics Letters*, vol. 35, no. 11, 2018, doi: 10.1088/0256-307X/35/11/117501.
- [2] L. Savary and L. Balents, “Quantum spin liquids: a review,” *Reports on Progress in Physics*, vol. 80, no. 1, p. 16502, 2016.
- [3] Y. Li, P. Gegenwart, and A. A. Tsirlin, “Spin liquids in geometrically perfect triangular antiferromagnets,” *Journal of Physics: Condensed Matter*, vol. 32, no. 22, p. 224004, 2020.
- [4] Y. Li, S. Bachus, Y. Tokiwa, A. A. Tsirlin, and P. Gegenwart, “Gapped ground state in the zigzag pseudospin-1/2 quantum antiferromagnetic chain compound PrTiNbO₆,” *Phys Rev B*, vol. 97, no. 18, p. 184434, 2018.
- [5] Y. Li *et al.*, “Partial Up-Up-Down Order with the Continuously Distributed Order Parameter in the Triangular Antiferromagnet TmMgGaO₄,” *Phys Rev X*, vol. 10, no. 1, Jan. 2020, doi: 10.1103/PhysRevX.10.011007.
- [6] C. Liu, C. J. Huang, and G. Chen, “Intrinsic quantum Ising model on a triangular lattice magnet TmMgGaO₄,” *Phys Rev Res*, vol. 2, no. 4, Oct. 2020, doi: 10.1103/PhysRevResearch.2.043013.
- [7] Y. Jiang and T. Emig, “String Picture for a Model of Frustrated Quantum Magnets and Dimers,” *Phys. Rev. Lett.*, vol. 94, no. 11, p. 110604, Mar. 2005, doi: 10.1103/PhysRevLett.94.110604.
- [8] Z. Zhou, C. Liu, Z. Yan, Y. Chen, and X.-F. Zhang, “Quantum dynamics of topological strings in a frustrated Ising antiferromagnet,” *npj Quantum Mater.*, vol. 7, no. 1, p. 60, 2022.
- [9] J. Nagl *et al.*, “Excitation spectrum and spin Hamiltonian of the frustrated quantum Ising magnet Pr₃BWO₉,” *Phys Rev Res*, vol. 6, no. 2, Apr. 2024, doi: 10.1103/PhysRevResearch.6.023267.
- [10] S. Zheng *et al.*, “Exchange-renormalized crystal field excitations in the quantum Ising magnet KTmSe₂,” *Phys Rev B*, vol. 108, no. 5, p. 54435, 2023.
- [11] J. Chaloupka, “Emergent transverse-field Ising model in d⁴ spin-orbit Mott insulators,” *Phys Rev B*, vol. 109, no. 2, p. L020403, 2024.
- [12] M. Moreno-Cardoner, H. Perrin, S. Paganelli, G. De Chiara, and A. Sanpera, “Case study of the uniaxial anisotropic spin-1 bilinear-biquadratic Heisenberg model on a triangular lattice,” *Phys. Rev. B*, vol. 90, no. 14, p. 144409, Oct. 2014, doi: 10.1103/PhysRevB.90.144409.

- [13] U. F. P. Seifert and L. Savary, “Phase diagrams and excitations of anisotropic $S=1$ quantum magnets on the triangular lattice,” *Phys. Rev. B*, vol. 106, no. 19, p. 195147, Nov. 2022, doi: 10.1103/PhysRevB.106.195147.
- [14] S. Hayami and K. Hattori, “Multiple- q Dipole–Quadrupole Instability in Spin-1 Triangular-lattice Systems,” *J Physical Soc Japan*, vol. 92, no. 12, p. 124709, 2023.
- [15] K. Hattori and H. Tsunetsugu, “Antiferro quadrupole orders in non-kramers doublet systems,” *J Physical Soc Japan*, vol. 83, no. 3, Mar. 2014, doi: 10.7566/JPSJ.83.034709.
- [16] T. Yanagisawa *et al.*, “Quadrupolar susceptibility and magnetic phase diagram of $\text{PrNi}_2\text{Cd}_{20}$ with non-Kramers doublet ground state,” *Philosophical Magazine*, vol. 100, no. 10, pp. 1268–1281, May 2020, doi: 10.1080/14786435.2019.1709912.
- [17] T. Onimaru and H. Kusunose, “Exotic quadrupolar phenomena in non-Kramers doublet systems - The cases of $\text{PrT}_2\text{Zn}_{20}$ ($T = \text{Ir, Rh}$) and $\text{PrT}_2\text{Al}_{20}$ ($T = \text{V, Ti}$),” Aug. 15, 2016, *Physical Society of Japan*. doi: 10.7566/JPSJ.85.082002.
- [18] C. Liu, Y. D. Li, and G. Chen, “Selective measurements of intertwined multipolar orders: Non-Kramers doublets on a triangular lattice,” *Phys Rev B*, vol. 98, no. 4, Jul. 2018, doi: 10.1103/PhysRevB.98.045119.
- [19] Y. Shen *et al.*, “Intertwined dipolar and multipolar order in the triangular-lattice magnet TmMgGaO_4 ,” *Nat Commun*, vol. 10, no. 1, p. 4530, 2019.
- [20] N. Tang *et al.*, “Spin–orbital liquid state and liquid–gas metamagnetic transition on a pyrochlore lattice,” *Nat Phys*, vol. 19, no. 1, pp. 92–98, 2023.
- [21] P. Thalmeier and A. Akbari, “Induced quantum magnetism in crystalline electric field singlet ground state models: Thermodynamics and excitations,” *Phys Rev B*, vol. 109, no. 11, Mar. 2024, doi: 10.1103/PhysRevB.109.115110.
- [22] B. Grover, “Dynamical properties of induced-moment systems,” *Physical Review*, vol. 140, no. 6A, p. A1944, 1965.
- [23] R. J. Birgeneau, J. Als-Nielsen, and E. Bucher, “VoLUMs 27, NUMBER 22 PHYSICAL REVIEW LETTERS 29.”
- [24] D. 8 Mc%han, C. Vettier, R. Youngblood, and G. Shirane, “Neutron scattering study of pressure-induced antiferromagnetism in PrSb .”
- [25] R. Moessner and S. L. Sondhi, “Ising models of quantum frustration,” *Phys Rev B*, vol. 63, no. 22, p. 224401, 2001.
- [26] Z. Hu *et al.*, “Evidence of the Berezinskii-Kosterlitz-Thouless phase in a frustrated magnet,” *Nat Commun*, vol. 11, no. 1, p. 5631, 2020.
- [27] H. Li *et al.*, “Kosterlitz-Thouless melting of magnetic order in the triangular quantum Ising material TmMgGaO_4 ,” *Nat Commun*, vol. 11, no. 1, p. 1111, 2020.

- [28] G. Chen, “Intrinsic transverse field in frustrated quantum Ising magnets: Physical origin and quantum effects,” *Phys Rev Res*, vol. 1, no. 3, Dec. 2019, doi: 10.1103/PhysRevResearch.1.033141.
- [29] R. Moessner, S. L. Sondhi, and P. Chandra, “Two-Dimensional Periodic Frustrated Ising Models in a Transverse Field,” *Phys. Rev. Lett.*, vol. 84, no. 19, pp. 4457–4460, May 2000, doi: 10.1103/physrevlett.84.4457.
- [30] G. H. Wannier, “Antiferromagnetism. The Triangular Ising Net,” *Phys. Rev.*, vol. 79, no. 2, pp. 357–364, Jul. 1950, doi: 10.1103/physrev.79.357.
- [31] G. Bastien *et al.*, “A frustrated antipolar phase analogous to classical spin liquids,” *arXiv preprint arXiv:2405.19859*, 2024, [Online]. Available: <https://arxiv.org/abs/2405.19859>
- [32] M. Ashtar *et al.*, “REZnAl₁₁O₁₉ (RE = Pr, Nd, Sm-Tb): A new family of ideal 2D triangular lattice frustrated magnets,” *J Mater Chem C Mater*, vol. 7, no. 32, pp. 10073–10081, 2019, doi: 10.1039/c9tc02643f.
- [33] M. Ashtar *et al.*, “Synthesis, structure and magnetic properties of rare-earth REMgAl₁₁O₁₉ (RE = Pr, Nd) compounds with two-dimensional triangular lattice,” *J Alloys Compd*, vol. 802, pp. 146–151, Sep. 2019, doi: 10.1016/j.jallcom.2019.06.177.
- [34] D. Ni and R. J. Cava, “Ferrites without iron as potential quantum materials,” *Progress in Solid State Chemistry*, vol. 66, p. 100346, 2022.
- [35] H. Bu *et al.*, “Gapless triangular-lattice spin-liquid candidate PrZnAl₁₁O₁₉,” *Phys. Rev. B*, vol. 106, no. 13, p. 134428, Oct. 2022, doi: 10.1103/PhysRevB.106.134428.
- [36] Z. Ma *et al.*, “Possible gapless quantum spin liquid behavior in the triangular-lattice Ising antiferromagnet PrMgAl₁₁O₁₉,” *Phys Rev B*, vol. 109, no. 16, Apr. 2024, doi: 10.1103/PhysRevB.109.165143.
- [37] Y. Cao *et al.*, “Synthesis, disorder and Ising anisotropy in a new spin liquid candidate PrMgAl₁₁O₁₉,” *Materials Futures*, vol. 3, no. 3, Sep. 2024, doi: 10.1088/2752-5724/ad4a93.
- [38] N. Li *et al.*, “Ising-type quantum spin liquid state in PrMgAl₁₁O₁₉,” Jul. 2024, [Online]. Available: <http://arxiv.org/abs/2407.11167>
- [39] C. Tu, Z. Ma, H. Wang, Y. Jiao, D. Dai, and S. Li, “Gapped quantum spin liquid in a triangular-lattice Ising-type antiferromagnet PrMgAl₁₁O₁₉,” Jul. 2024, [online]. Available: <http://arxiv.org/abs/arXiv:2407.20081>
- [40] Y. Qin *et al.*, “Field-tuned quantum effects in a triangular-lattice Ising magnet,” *Sci Bull (Beijing)*, vol. 67, no. 1, pp. 38–44, 2022.
- [41] J. Xing *et al.*, “Crystal synthesis and frustrated magnetism in triangular lattice CsRESe₂ (RE= La–Lu): Quantum spin liquid candidates CsCeSe₂ and CsYbSe₂,” *ACS Mater Lett*, vol. 2, no. 1, pp. 71–75, 2019.

- [42] N. Kabeya *et al.*, “Competing Exchange Interactions in Lanthanide Triangular Lattice Compounds LnZn_3P_3 (Ln= La–Nd, Sm, Gd),” *J Physical Soc Japan*, vol. 89, no. 7, p. 74707, 2020.
- [43] L. Wang, Z. Ouyang, T. Xiao, Z. Li, and Z. Tian, “Synthesis, structure and magnetism of $\text{RTa}_7\text{O}_{19}$ (R= Pr, Sm, Eu, Gd, Dy, Ho) with perfect triangular lattice,” *J Alloys Compd*, vol. 937, p. 168390, 2023.
- [44] A. N. Rutherford, C. Xing, H. Zhou, Q. Huang, and S. Calder, “Magnetic properties of $\text{RE}_2\text{O}_2\text{CO}_3$ (RE = Pr, Nd, Gd, Tb, Dy, Ho, Er, Yb) with a rare earth-bilayer of triangular lattice,” Jul. 2024, [Online]. Available: <http://arxiv.org/abs/2407.08606>
- [45] S. Guo, T. Kong, and R. J. Cava, “ $\text{NaBaR}(\text{BO}_3)_2$ (R= Dy, Ho, Er and Tm): structurally perfect triangular lattice materials with two rare earth layers,” *Mater Res Express*, vol. 6, no. 10, p. 106110, 2019.
- [46] S. Zheng *et al.*, “Interplay between crystal field and magnetic anisotropy in the triangular-lattice antiferromagnet NaTmTe_2 ,” *Phys Rev B*, vol. 109, no. 7, p. 75159, 2024.
- [47] T. Arh *et al.*, “The Ising triangular-lattice antiferromagnet neodymium heptatantalate as a quantum spin liquid candidate,” *Nat Mater*, vol. 21, no. 4, pp. 416–422, 2022.
- [48] A. Kahn, A.-M. Lejus, M. Madsac, J. Thery, D. Vivien, and J. C. Bernier, “Preparation, structure, optical, and magnetic properties of lanthanide aluminate single crystals ($\text{LnMgAl}_{11}\text{O}_{19}$),” *J Appl Phys*, vol. 52, no. 11, pp. 6864–6869, 1981.
- [49] D. Staško *et al.*, “The synthesis of the rare earth $\text{A}_2\text{Zr}_2\text{O}_7$ single crystals by simplified laser-heated floating hot zone and pedestal methods,” *Mater Today Chem*, vol. 39, Jul. 2024, doi: 10.1016/j.mtchem.2024.102153.
- [50] M. Klicpera *et al.*, “Magnetic frustration in rare-earth zirconates $\text{A}_2\text{Zr}_2\text{O}_7$, the case of laser heated pedestal method synthesised A = Er, Tm, Yb, and Lu single crystals,” *J Alloys Compd*, vol. 978, Mar. 2024, doi: 10.1016/j.jallcom.2024.173440.

Figures

Fig. 1

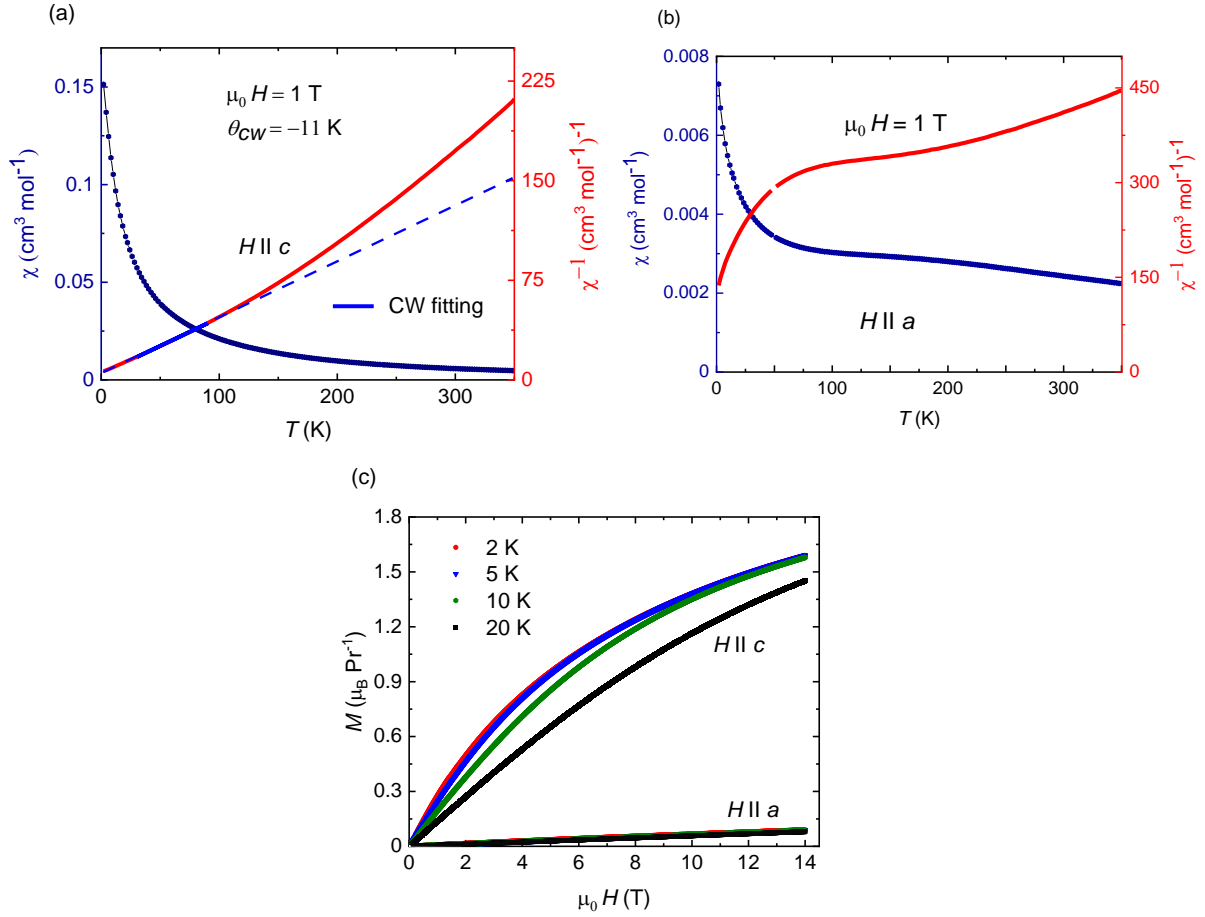


FIG. 1: Magnetic susceptibility and inverse susceptibility measured with an external magnetic field $\mu_0 H = 1$ T, when H is applied parallel to the c -axis (a), and perpendicular to the c -axis (b). The blue line in (a) represents the Curie-Weiss (CW) fitting of the inverse susceptibility in the temperature range of 30-80 K, yielding a Curie-Weiss temperature (θ_{CW}) of -11 K. (c) Isothermal magnetization as a function of the field at different temperatures between 2 K and 30 K for fields applied in the ab -plane and along the c -axis, demonstrating significant magnetic anisotropy in the system.

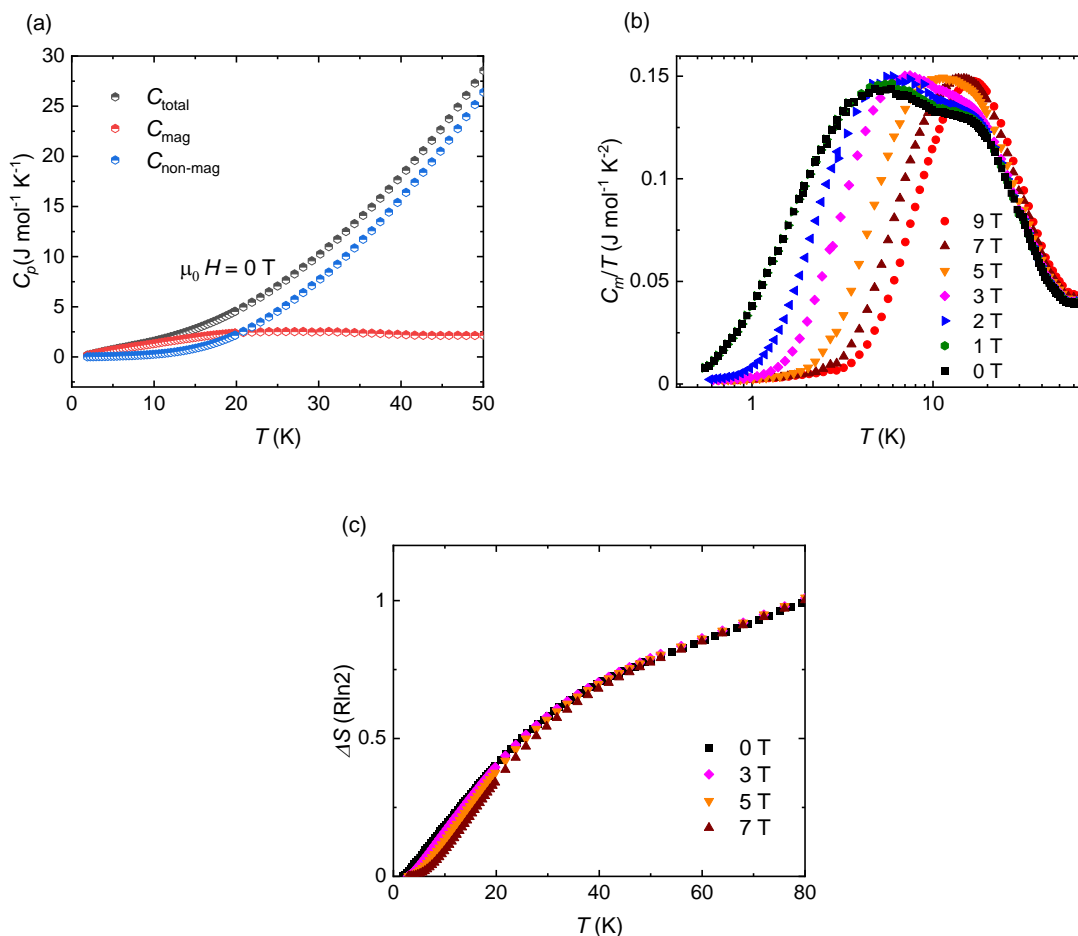
Fig. 2

FIG. 2: Specific heat measurements for PrMgAl₁₁O₁₉. (a) Total specific heat (C_p) as a function of temperature, compared with the non-magnetic analog LaMgAl₁₁O₁₉ ($C_{\text{non-m}}$) to isolate the magnetic contribution (C_m). (b) C_m/T as a function of T , showing a broad hump that shifts to higher temperatures with an increasing applied magnetic field. (c) Magnetic entropy change (ΔS) as a function of temperature, approaching $R \ln 2$ around 80 K.

Fig. 3

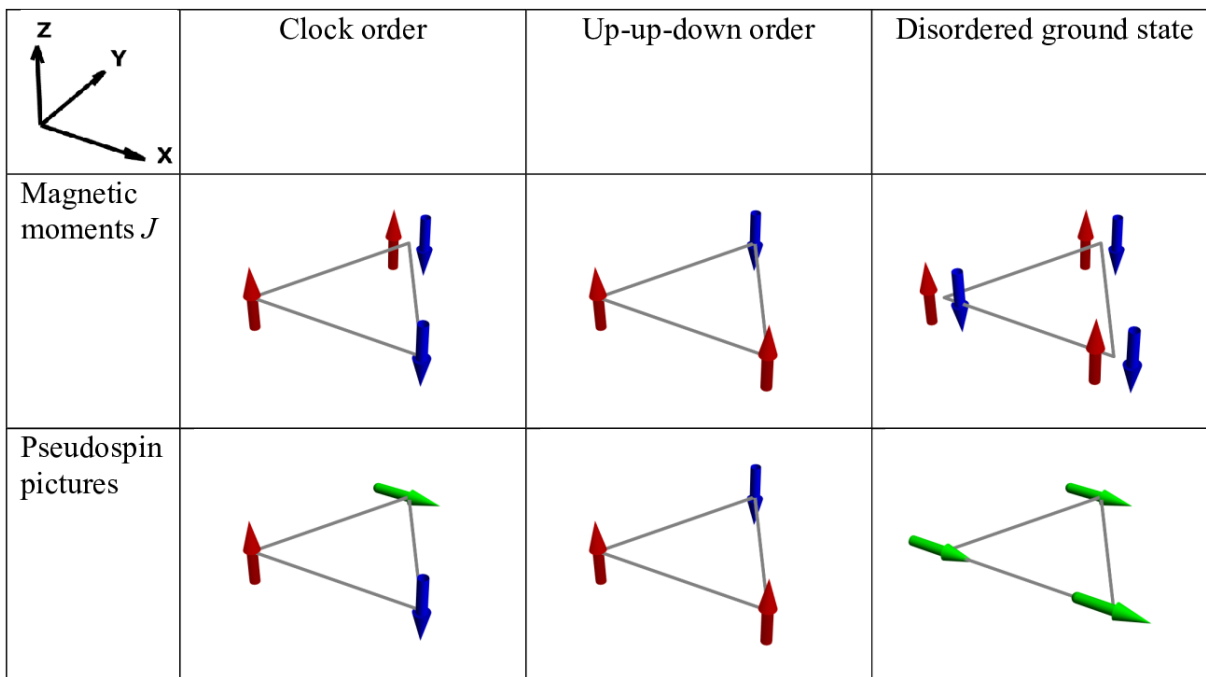


FIG. 3: Schematic view of magnetic phases in competition in triangular magnets with non-Kramers magnetic ions such as Pr^{3+} or Tm^{3+} . The superposition $|0\rangle = |J_z = +4\rangle + |J_z = -4\rangle$ is represented by both a moment up and a moment down or in the pseudospin picture by a pseudospin pointing towards the transverse direction x . These three phases were located on the $h - H$ phase diagram by previous theoretical work [6].

Fig. 4

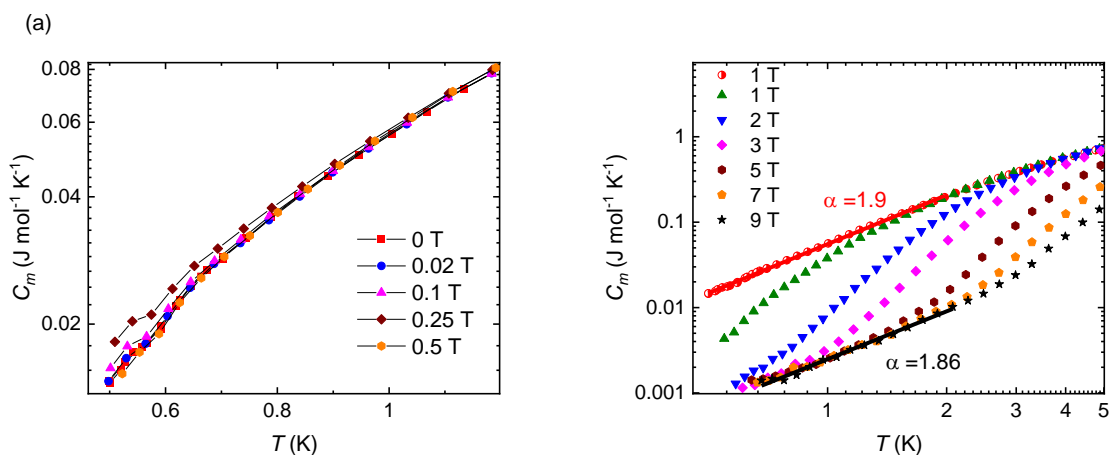


FIG. 4: Magnetic contribution C_m to the specific heat in or $\text{PrMgAl}_{11}\text{O}_{19}$ as a function of temperature under a magnetic field up to 0.5 T in (a) and up to 9T in (b). The solid lines indicate power law fitting.